Search for Exclusive $b \to u$ Semileptonic Decays of B Mesons

A. Bean,[1] J. Gronberg,[1] R. Kutschke,[1] S. Menary,[1] R. J. Morrison,[1] H. N. Nelson,[1] J. D. Richman,[1] H. Tajima,[1] D. Schmidt,[1] D. Sperka,[1] M. S. Witherell,[1] M. Procario,[2] S. Yang,[2] R. Ballest,[3] M. Daoudi,[3] W. T. Ford,[3] D. R. Johnson,[3] K. Lingel,[3] M. Lohner,[3] P. Rankin,[3] J. G. Smith,[3] J. P. Alexander,[4] C. Bebek,[4] K. Berkelman,[4] D. Besson,[4] T. E. Browder,[4] D. G. Cassel,[4] H. A. Cho,[4] D. M. Coffman,[4] P. S. Drell,[4] R. Ehrlich,[4] R. S. Galik,[4] M. Garcia-Sciveres,[4] B. Geiser,[4] B. Gittelman,[4] S. W. Gray,[4] D. L. Hartill,[4] B. K. Heltsley,[4] K. Honscheid,[4] C. D. Jones,[4] J. Kandaswamy,[4] N. Katayama,[4] P. C. Kim,[4] D. L. Kreinick,[4] G. S. Ludwig,[4] J. Masui,[4] J. Mevissen,[4] N. B. Mistry,[4] C. R. Ng,[4] E. Nordberg,[4] M. Ogg,[4],[a] C. O'Grady,[4] J. R. Patterson,[4] D. Peterson,[4] D. Riley,[4] M. Sapper,[4] M. Selen,[4] H. Worden,[4] M. Worris,[4] F. Würthwein,[4] P. Avery,[5] A. Freyberger,[5] J. Rodriguez,[5] R. Stephens,[5] J. Yelton,[5] D. Cinabro,[6] S. Henderson,[6] K. Kinoshita,[6] T. Liu,[6] M. Saulnier,[6] R. Wilson,[6] H. Yamamoto,[6] A. J. Sadoff,[7] R. Ammar,[8] S. Ball,[8] P. Baringer,[8] D. Coppage,[8] N. Copty,[8] R. Davis,[8] N. Hancock,[8] M. Kelly,[8] N. Kwak,[8] H. Lam,[8] Y. Kubota,[9] M. Lattery,[9] J. K. Nelson,[9] S. Patton,[9] D. Perticone,[9] R. Poling,[9] V. Savinov,[9] S. Schrenk,[9] R. Wang,[9] M. S. Alam,[10] I. J. Kim,[10] B. Nemati,[10] J. J. O'Neill,[10] V. Romero,[10] H. Severini,[10] C. R. Sun,[10] M. M. Zoeller,[10] G. Crawford,[11] R. Fulton,[11] K. K. Gan,[11] H. Kagan,[11] R. Kass,[11] J. Lee,[11] R. Malchow,[11] F. Morrow,[11] Y. Skovpen,[11],[b] M. Sung,[11] C. White,[11] J. Whitmore,[11] P. Wilson,[11] F. Butler,[12] X. Fu,[12] G. Kalbfleisch,[12] M. Lambrecht,[12] W. R. Ross,[12] P. Skubic,[12] J. Snow,[12] P. L. Wang,[12] M. Wood,[12] D. Bortoletto,[13] D. N. Brown,[13] J. Dominick,[13] R. L. McIlwain,[13] T. Miao,[13] D. H. Miller,[13] M. Modesitt,[13] S. F. Schaffner,[13] E. I. Shibata,[13] I. P. J. Shipsey,[13] P. N. Wang,[13] M. Battle,[14] J. Ernst,[14] H. Kroha,[14] S. Roberts,[14] K. Sparks,[14] E. H. Thorndike,[14] C. H. Wang,[14] S. Sanghera,[15] T. Skwarnicki,[15] R. Stroynowski,[15] M. Artuso,[16] M. Goldberg,[16] N. Horwitz,[16] R. Kennett,[16] G. C. Moneti,[16] F. Muheim,[16] S. Playfer,[16] Y. Rozen,[16] P. Rubin,[16] S. Stone,[16] M. Thulasidas,[16] G. Zhu,[16] A. V. Barnes,[17] J. Bartelt,[17] S. E. Csorna,[17] Z. Egyed,[17] V. Jain,[17] P. Sheldon,[17] D. S. Akerib,[18] B. Barish,[18] M. Chadha,[18] S. Chan,[18] D. F. Cowen,[18] G. Eigen,[18] J. S. Miller,[18] J. Urheim,[18] A. J. Weinstein,[18] D. Acosta,[19] M. Athanas,[19] G. Masek,[19] B. Ong,[19] H. Paar,[19] and M. Sivertz[19]

(CLEO Collaboration)

[1]*University of California, Santa Barbara, California 93106*
[2]*Carnegie-Mellon University, Pittsburgh, Pennsylvania 15213*
[3]*University of Colorado, Boulder, Colorado 80309-0390*
[4]*Cornell University, Ithaca, New York 14853*
[5]*University of Florida, Gainesville, Florida 32611*
[6]*Harvard University, Cambridge, Massachusetts 02138*
[7]*Ithaca College, Ithaca, New York 14850*
[8]*University of Kansas, Lawrence, Kansas 66045*
[9]*University of Minnesota, Minneapolis, Minnesota 55455*
[10]*State University of New York at Albany, Albany, New York 12222*
[11]*Ohio State University, Columbus, Ohio 43210*
[12]*University of Oklahoma, Norman, Oklahoma 73019*
[13]*Purdue University, West Lafayette, Indiana 47907*
[14]*University of Rochester, Rochester, New York, 14627*
[15]*Southern Methodist University, Dallas, Texas 75275*
[16]*Syracuse University, Syracuse, New York, 13244*
[17]*Vanderbilt University, Nashville, Tennessee 37235*
[18]*California Institute of Technology, Pasadena, California 91125*
[19]*University of California at San Diego, La Jolla, California 92093*

(Received 21 December 1992)

Using a sample of 935000 $B\bar{B}$ pairs collected with the CLEO-II detector at the Cornell Storage Ring, we have obtained upper limits on the branching ratios for the $b \to u l^- \bar{\nu}$ processes $B^- \to \omega l^- \bar{\nu}$, $B^- \to \rho^0 l^- \bar{\nu}$, and $\bar{B}^0 \to \rho^+ l^- \bar{\nu}$. The combined result using the relationships among the widths for these three modes is $B(B^- \to \rho^0 l^- \bar{\nu}) < (1.6\text{–}2.7) \times 10^{-4}$ at 90% C.L., where the range of values is due to model dependence of the detection efficiencies. These measurements yield the limits $|V_{ub}/V_{cb}| < 0.08\text{–}0.13$.

PACS numbers: 13.20.Jf, 12.15.Ff, 14.40.Jz

The decays $B^- \to \omega l^- \bar{\nu}$, $B^- \to \rho^0 l^- \bar{\nu}$, and $\bar{B}^0 \to \rho^+ l^- \bar{\nu}$ correspond to the highly suppressed transition $b \to u l^- \bar{\nu}$. These processes are therefore sensitive to the standard model parameter V_{ub}, one of the smallest and least well measured elements of the Cabibbo-Kobayashi-Maskawa (CKM) quark-mixing matrix. Current knowledge of $|V_{ub}|$ is based on measurements [1] of the inclusive energy spectrum of leptons produced in B meson decay. In addition, the ARGUS Collaboration has presented preliminary evidence for a $B^- \to \rho^0 l^- \bar{\nu}$ signal [2].

In the $b \to u$ decay $B^- \to X_u l^- \bar{\nu}$, the hadronic system X_u can range over much of the light-quark hadron spectrum, and no single final state is expected to dominate. Theoretical models indicate that the branching ratios for the decays $B \to \rho(\omega) l^- \bar{\nu}$ should be among the largest of these rare processes. For example, $B^- \to \rho^0 l^- \bar{\nu}$ is predicted to account for 3.5% to 14% [3–5] of the inclusive $B^- \to X_u l^- \bar{\nu}$ rate. The three decay modes we have investigated are related. The two $B \to \rho l^- \bar{\nu}$ decays are connected by isospin symmetry in the hadronization process, and the ρ^0 and ω modes are expected, in the quark model, to have approximately equal rates,

$$\Gamma(\bar{B}^0 \to \rho^+ l^- \bar{\nu}) = 2\Gamma(B^- \to \rho^0 l^- \bar{\nu}) \simeq 2\Gamma(B^- \to \omega l^- \bar{\nu}). \quad (1)$$

(Throughout this paper, the charge-conjugate modes are implied.)

Our analysis uses 935000 $B\bar{B}$ pairs (923 pb^{-1}) collected with the CLEO-II detector [6] at the Cornell Electron Storage Ring (CESR). At the e^+e^- center-of-mass energy $\sqrt{s} = 10.58$ GeV, the hadronic cross section has a resonant component, due to production of the $\Upsilon(4S)$, and a nonresonant (continuum) component that is about 3 times larger. To study the continuum background, we use a 416 pb^{-1} data sample accumulated at $\sqrt{s} = 10.52$ GeV.

For $B \to \rho(\omega) l^- \bar{\nu}$, quark models predict that the spectrum of E_l (the lepton energy in the laboratory frame) peaks at 2.2 GeV, near the kinematic limit. By requiring $E_l \geq 2.0$ GeV, we suppress the dominant background, $b \to c l^- \bar{\nu}$, which has a substantially softer lepton-energy spectrum. All the models we have considered predict that the fraction of $B \to \rho(\omega) l^- \bar{\nu}$ decays with $E_l > 2.0$ GeV is large: 0.72 in ISGW [3], 0.68 in KS [4], and 0.52 in WSB [5].

The analysis consists of two main steps. We first select events whose characteristics are consistent with the presence of two B mesons, each nearly at rest, with one decaying into $\pi\pi l\nu$ or $\pi^+\pi^-\pi^0 l\nu$. We optimize the selection cuts separately in two lepton-energy regions, LOLEP, $2.0 \leq E_l < 2.3$ GeV, and HILEP, $E_l \geq 2.3$ GeV. Because the lepton-energy spectrum from $b \to c l^- \bar{\nu}$ falls off sharply around 2.3 GeV, the background in the LOLEP region is dominated by $b \to c l^- \bar{\nu}$ processes, whereas the background in the HILEP region is much smaller and is dominated by continuum events. In the second step of the analysis, we fit the resulting $\pi\pi(\pi^+\pi^-\pi^0)$ mass spectra to obtain limits on $B \to \rho(\omega) l^- \bar{\nu}$.

We divide the set of tracks in an event into two groups: those in the $\rho(\omega)l$ candidate (Y system) and those that remain (X system). In each event, all possible combinations are considered. We require the kinematics of the Y system to be consistent with the presence of an unobserved neutrino from the semileptonic decay of the B meson. Under this hypothesis, the constraint $m_\nu = 0$ allows us to compute the direction cosine between the Y system and the B, $\cos\theta_{B,Y} = (2E_B E_Y - m_B^2 - m_Y^2)/(2|\mathbf{p}_B||\mathbf{p}_Y|)$, which we require to satisfy $|\cos\theta_{B,Y}| \leq 1.0$. Here we also use the constraints $E_B = E_{\rm beam}$ and $|\mathbf{p}_B| = (E_{\rm beam}^2 - m_B^2)^{1/2}$. To increase the likelihood that the X system originates from the decay of the other B (B_X), we exploit the fact that, within resolution, the square of the mass of the unobserved decay products of the B_X must be positive or zero. We require

$$M_{\rm miss}^2(X) = (p_{B_X} - p_X)^2 = m_B^2 + m_X^2 - 2(E_{B_X}E_X - |\mathbf{p}_{B_X}||\mathbf{p}_X|\cos\theta_{B_X,X}) \quad (2)$$

to satisfy $-0.2 \leq M_{\rm miss}^2(X) \leq 5.0$ GeV^2. We again use the beam-energy constraint to define E_{B_X} and $|\mathbf{p}_{B_X}|$. For the X system, we assume that all charged tracks are pions and that all showers not matched to charged tracks are due to photons. Finally, we set the unknown quantity $\cos\theta_{B_X,X}$ to 1, which retains the largest number of signal events for a given cut on $M_{\rm miss}^2(X)$.

Table I gives the values of the remaining cuts, which depend on the decay channel and on the E_l region. Continuum events, unlike $\Upsilon(4S) \to B\bar{B}$ decays, have jetlike topologies and can be suppressed by analyzing the event shape. For each $\rho(\omega)l$ candidate, we cut on $\cos\theta_{\rm thr} \equiv \mathbf{n}_{X\,\rm thr} \cdot \mathbf{n}_{Y\,\rm thr}$, where $\mathbf{n}_{X(Y)\rm thr}$ is the thrust axis direction for tracks in the X (Y) system. Since the two B's have $J = 0$ and are nearly at rest ($\beta \approx 0.06$), the distribution of $\cos\theta_{\rm thr}$ is uniform for signal events. For continuum events, the $\cos\theta_{\rm thr}$ distribution peaks strongly at ± 1. To further suppress the continuum, we cut on the Fox-Wolfram [7] event-shape variable $R_2 \equiv H_2/H_0$.

TABLE I. Analysis cuts for $B \to \rho(\omega) l^- \bar{\nu}$.

V	R_2	$\lvert\cos\theta_{\rm thr}\rvert$	E_{π^0} (GeV)	$\sum \mathbf{p}\cdot\mathbf{n}_Y$ (GeV)	$E_{\rho(\omega)l}$ (GeV)
			HILEP ($E_l \geq 2.3$ GeV)		
ω	< 0.30	< 0.7	≥ 0.20	≥ -0.30	≥ 3.3
ρ^0	< 0.25	< 0.7	···	≥ -0.20	≥ 3.2
ρ^+	< 0.25	< 0.7	≥ 0.35	≥ -0.20	≥ 3.0
			LOLEP ($2.0 \leq E_l < 2.3$ GeV)		
ω	< 0.30	< 0.8	≥ 0.25	≥ -0.20	≥ 3.3
ρ^0	< 0.30	< 0.8	···	≥ -0.20	≥ 3.0
ρ^+	< 0.30	< 0.8	≥ 0.35	≥ -0.20	≥ 3.0

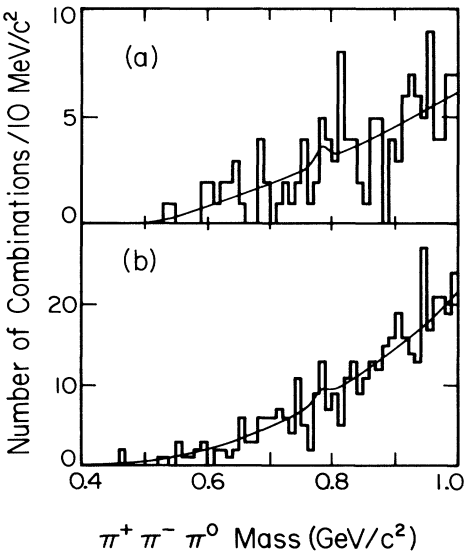

FIG. 1. The $\pi^+\pi^-\pi^0$ invariant mass spectra for $\pi^+\pi^-\pi^0 l$ combinations that pass (a) the HILEP cuts and (b) the LOLEP cuts. The curves are described in the text.

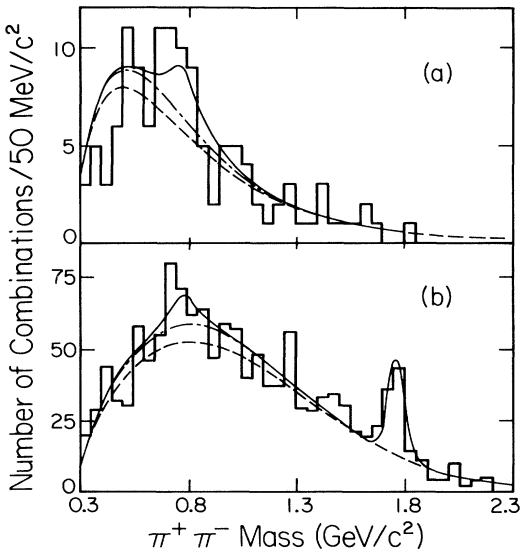

FIG. 2. The $\pi^+\pi^-$ invariant mass spectra for $\pi^+\pi^-$ combinations that pass (a) the HILEP cuts and (b) the LOLEP cuts. The curves are described in the text.

For signal events, the sum of the momenta of the $Y+\nu$ system and of the B_X will be zero. Although the direction of the B that decays semileptonically is unknown, it is possible to calculate its momentum component along the Y system's direction of motion ($\mathbf{n}_Y$). The total momentum along $\mathbf{n}_Y$ is $\sum \mathbf{p}\cdot\mathbf{n}_Y = \mathbf{p}_X\cdot\mathbf{n}_Y + |\mathbf{p}_B|\cos_{B,Y}$, where we have used the measured momentum of the X system to approximate that of the B_X. For the signal, the distribution of $\sum \mathbf{p}\cdot\mathbf{n}_Y$ is centered at zero, whereas the backgrounds have strongly skewed distributions.

To suppress combinatorial background, we require the π^0 energy to exceed a minimum value. We also cut on the sum of the lepton and vector meson energies, $E_{\rho(\omega)l}$. For the $B^- \to \omega l^- \bar{\nu}$ channel, we cut on the ω decay amplitude: $A(\omega \to \pi^+\pi^-\pi^0) \propto |\mathbf{p}_{\pi^+} \times \mathbf{p}_{\pi^-}|$, where the pion momenta are measured in the ω rest frame. We require that $|A|^2$ be at least 0.4 of its maximum value.

Figure 1 shows the $\pi^+\pi^-\pi^0$ mass spectra after all cuts from the ω analyses have been applied; Figs. 2 and 3 show the corresponding $\pi^+\pi^-$ and $\pi^+\pi^0$ mass spectra. None shows a clear ω or ρ signal. The $\pi^+\pi^-$ mass spectrum for the $B^- \to \rho^0 l^- \bar{\nu}$ LOLEP sample shows a small peak near 1.7 GeV, due to $D^0 \to K^-\pi^+$ decays in which the kaon is misidentified as a pion.

To set limits on the number of ω's and ρ's in these spectra, we perform binned maximum likelihood fits. For the ω analysis, we use a Breit-Wigner line shape convoluted with a Gaussian ($\sigma = 8$ MeV) to describe the ω and a second-order Chebyshev polynomial to describe the background; the sum of these terms is represented by the solid lines in Fig. 1. The ω mass resolution is verified using the inclusive ω signal observed in CLEO-II data. Because the ω is narrow, these fits are insensitive to the background shape.

The fits to the $\pi\pi$ mass spectra incorporate three separate background terms in addition to the ρ signal, which is parametrized by a ρ Breit-Wigner function. In HILEP, these terms are (1) a term whose shape and normalization is fixed from a fit to the continuum data sample, after the same cuts are applied; (2) a smooth function, which is allowed to vary in both shape and normalization, to represent any remaining background, from

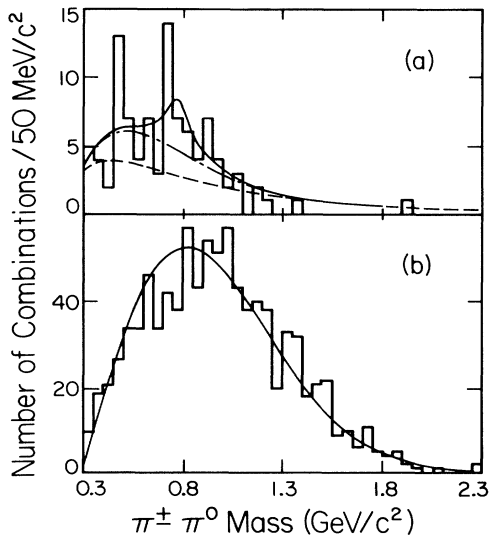

FIG. 3. The $\pi^\pm\pi^0$ invariant mass spectra for $\pi^\pm\pi^0$ combinations that pass (a) the HILEP cuts and (b) the LOLEP cuts. The curves are described in the text.

TABLE II. Efficiencies and fit results (ISGW model). Positive central values cannot be interpreted as evidence for a signal, because there may remain ρ or ω contributions from background sources. Divide the ρ^+ results by 2 (isospin) to compare with ρ^0. The errors are discussed in the text.

V	$N(V)$	ϵ (%)	$\frac{B(B\to Vl^-\bar{\nu})}{10^{-4}}$	Limit/10^{-4} (90% C.L.)
		HILEP ($E_l \geq 2.3$ GeV)		
ω	2.1 ± 4.3	2.4	$0.5\pm1.1\pm0.1$	<2.1
ρ^0	$12\pm6\pm10$	7.1	$0.9\pm0.5\pm0.8$	<2.1
ρ^+	$17\pm5\pm9$	4.1	$2.2\pm0.7\pm1.2$	<4.1
		LOLEP ($2.0\leq E_l<2.3$ GeV)		
ω	3.6 ± 6.6	1.6	$1.4\pm2.5\pm0.3$	<5.0
ρ^0	$56\pm22\pm35$	8.1	$3.7\pm1.5\pm2.4$	<7.5
ρ^+	$-59\pm30\pm93$	5.4	$-5.8\pm3.0\pm9.3$	<12.9

$b\to cl^-\bar{\nu}$ or from other sources; and (3) a smooth function, whose shape is fixed by the *signal* Monte Carlo, which represents the combinatorial background present in signal events when the Y system contains decay products from both B mesons. The normalization of the third term is fixed relative to the area of the ρ Breit-Wigner function using the signal Monte Carlo. In Figs. 2(a) and 3(a), the dashed curves show the sum of terms (1) and (2), the dot-dashed curves represent the sum of all three background terms, and the solid curves represent the sum of the signal term plus all background terms. In contrast to the ω channel, systematic errors arise here from the uncertainties in the background shape and normalization. In the HILEP analysis the dominant contributions are due to uncertainty in the ρ combinatorial background shape and in the shape and normalization of the measured continuum background.

In the LOLEP analysis, the dominant background, $b\to cl^-\bar{\nu}$, cannot be independently measured in data, and the background is modeled differently. Our fit includes (1) a smooth function, whose normalization and shape are both allowed to vary, to represent the sum of $b\to cl^-\bar{\nu}$ and continuum processes; (2) a Gaussian in the $\pi^+\pi^-$ channel to represent the D^0 satellite peak; and (3) a combinatorial background function (similar to that described in the ρ HILEP fit), which we obtain from the signal Monte Carlo. In Fig. 2(b) the dashed curve shows term (1); the dot-dashed curve represents the sum of terms (1) and (3); and the solid curve represents the sum of the signal term plus the backgrounds. In Fig. 3(b) the solid curve represents term (1) only, with no contribution from signal or term (3). The best fit, however, yields a small negative signal. The dominant systematic errors in the LOLEP analysis arise from uncertainty in the shape of the $b\to cl^-\bar{\nu}$ background, which is studied using both wrong-sign events ($\rho^\pm l^\pm$) and Monte Carlo.

Table II gives central values and limits for each mode, assuming efficiencies from a Monte Carlo simulation using the ISGW model. The first error on the yield $N(V)$ is statistical, whereas the second is a systematic error that includes the uncertainty in the background shapes. The errors on the branching ratio are statistical and systematic, where the systematic error includes the 17% uncertainty in the efficiency. With the relationships given in Eq. (1), we compute a weighted average [8] using all channels, which we present for each model in Table III.

TABLE III. Combined upper limits for three models. As in Table II, positive central values cannot be interpreted as evidence for a signal.

Model	$\frac{B(B^-\to V^0l^-\bar{\nu})}{10^{-4}}$	Limit/10^{-4} (90% C.L.)	$\lvert V_{ub}/V_{cb}\rvert$ (90% C.L.)
ISGW	1.0 ± 0.5	<1.6	<0.13
WSB	1.6 ± 0.9	<2.7	<0.10
KS	1.3 ± 0.7	<2.3	<0.08

In conclusion, we find, for the set of models considered,

$$B(B^-\to V^0l^-\bar{\nu})<(1.6\text{–}2.7)\times10^{-4} \text{ at } 90\% \text{ C.L.}, \quad (3)$$

where l indicates either an electron or a muon but not both. Similarly, V^0 represents a neutral vector meson, either ρ^0 or ω. Our result is inconsistent at the 2.3σ level with a preliminary ARGUS measurement [2], $B(B^-\to\rho^0l^-\bar{\nu})=(11.3\pm3.6\pm2.7)\times10^{-4}$, where the ISGW model was used to obtain the efficiency. An earlier ARGUS analysis [1(d)] obtained $B(B^-\to\rho^0l^-\bar{\nu})<11\times10^{-4}$ at 90% C.L. Using the partial width predictions from the theoretical models in terms of $|V_{ub}|$, and assuming [9] $\tau_B\times|V_{cb}|^2=1.29$ ps$\times(0.041)^2$, we obtain limits on $|V_{ub}/V_{cb}|$ (Table III) ranging from 0.08 to 0.13. This result is consistent with the new preliminary CLEO-II inclusive measurement of $|V_{ub}/V_{cb}|=0.05$–0.12 [1(a)]. It favors the lower part of the range allowed from the earlier inclusive measurements of CLEO [1(b)] (0.09–0.15) and ARGUS [1(d)] (0.11–0.20).

We gratefully acknowledge the effort of the CESR staff in providing us with excellent luminosity and running conditions. J.P.A. and P.S.D. thank the PYI program of the NSF, I.P.J.S. thanks the YI program of the NSF, K.H. thanks the Alexander von Humboldt Stiftung, G.E. thanks the Heisenberg Foundation, K.K.G. and A.J.W. thank the SSC Fellowship program of TNRLC, J.D.R., K.K.G., H.N.N., and H.Y. thank the OJI program of DOE, and R.P. and P.R. thank the A. P. Sloan Foundation for support. This work was supported by the National Sciencie Foundation and the U.S. Department of Energy.

[a]Permanent address: Carleton University, Ottawa, Canada.

[b]Permanent address: Institute of Nuclear Physics, Novosibirsk, Russia.

[1] (a) CLEO Collaboration, F. Muheim *et al.*, in "Confirmation of Charmless Semileptonic Decays of B Mesons," Proceedings of the Seventh Meeting of the American Physical Society Division of Particles and Fields, Fermilab, 10–14 November 1992 (to be published); (b) CLEO Collaboration, R. Fulton *et al.*, Phys. Rev. Lett. **64**, 16 (1990); (c) ARGUS Collaboration, H. Albrecht *et al.*, Phys. Lett. B **234**, 409 (1990); (d) ARGUS Collaboration, H. Albrecht *et al.*, Phys. Lett. B **255**, 297 (1991).

[2] ARGUS Collaboration, M. Paulini *et al.*, in *Proceedings of the Joint International Symposium & Europhysics Conference on High Energy Physics*, edited by S. Hegarty, K. Potter, and E. Quercigh (World Scientific, Singapore, 1992), p. 592.

[3] N. Isgur, D. Scora, B. Grinstein, and M. Wise, Phys. Rev. D **39**, 799 (1989).

[4] J. G. Körner and G. A. Schuler, Z. Phys. C **46**, 93 (1990).

[5] M. Wirbel, B. Stech, and M. Bauer, Z. Phys. C **29**, 637 (1985).

[6] CLEO Collaboration, Y. Kubota *et al.*, Nucl. Instrum. Methods Phys. Res., Sect. A **320**, 66 (1992).

[7] G. Fox and S. Wolfram, Phys. Rev. Lett. **41**, 1581 (1978).

[8] The weights for the average are computed using only the uncorrelated part of the errors. The fractional correlated error is then applied to final central value and added in quadrature with the uncorrelated error.

[9] Particle Data Group, K. Hikasa *et al.*, Phys. Rev. D **45**, Part II (1992).